Original Article

Moisture dependent tensile and creep behaviour of multi-wall carbon nanotube and carbon fibre reinforced, injection moulded polyamide 6 matrix multi-scale composites

Roland Petrény [a], *László Mészáros* [a,b,*]

[a] *Department of Polymer Engineering, Faculty of Mechanical Engineering, Budapest University of Technology and Economics, Műegyetem rkp. 3., H-1111 Budapest, Hungary*
[b] *MTA—BME Research Group for Composite Science and Technology, 1111, Műegyetem rkp. 3, Budapest, Hungary*

ARTICLE INFO

ABSTRACT

In this study the creep behaviour and its dependence on moisture content in injection moulded hybrid composites reinforced with carbon fibres and carbon nanotubes was investigated. The tensile tests and the scanning electron microscope images confirmed that the presence of carbon fibres helped the uniform distribution of carbon nanotubes in the matrix. In the composites reinforced only with carbon fibres, the creep rate was lower than in any of the composites reinforced with only carbon nanotubes. Synergistic effects were observed when carbon nanotubes were added to the composite besides the carbon fibres: the creep rate was even lower and decreased with the increase in nanotube content. In the composites only reinforced with carbon nanotubes, crystallinity decreased, and moisture absorption increased with increasing nanotube content, but in the hybrid composites, the decrease in crystallinity and moisture absorption was much lower, thus the disadvantageous effect of moisture on the creep rate was much smaller in the hybrid composites.

1. Introduction

Over the past 10—15 years, carbon nanotube reinforced polymer composites have become more and more prominent, but their breakthrough has so far lagged behind. This may be due to the fact that the mechanical properties of nanocomposites produced by mass production technologies have not improved considerably compared to conventional composites. In the case of the widespread, fibre-reinforced composites, even the mathematical modelling of their mechanical behaviour is extensively researched, but only little information is available about nanocomposites including their long-term behaviour and the effects of environmental parameters [1—5].

The mechanical properties of composites are significantly determined by the size of the interface between the fibre and the matrix; reinforcing is most effective when the reinforcing material adheres to the matrix on the largest possible surface. In the early 2000s, nanoscale reinforcements came to the fore, due to their extremely high surface/volume ratio. A very

---

promising nanoscale reinforcement is carbon nanotubes, which have a surface/volume ratio of a few tens of thousands $\frac{1}{m}$. Compared to this, conventionally used short carbon fibres have only a few hundreds $\frac{1}{m}$ of surface/volume ratio. In addition, nanoscale reinforcing materials have outstanding mechanical properties, well beyond those of conventional reinforcements of composites. Multi-wall carbon nanotubes (MWCNT), have approximately 200—900 GPa tensile modulus, 14 GPa bending strength and 20—63 GPa tensile strength [6—10].

However, mechanical properties of carbon nanotube reinforced composites are highly dependent on the degree of dispersion of the nanotubes. Carbon nanotubes tend to adhere strongly to each other and usually form large aggregates during their production, thus during the processing of the composite material, nanotubes tend to remain in this aggregated form. This may lead to nanotubes functioning as stress concentration centres instead of reinforcing. To achieve uniform dispersion of nanotubes, a large variety of methods have been developed in the past few years, most of which are based on the chemical surface modification of nanotubes that may disrupt the regular structure of nanotubes, and often are quite expensive which limits the widespread use of nanotube-reinforced composites [1,11—13].

Uniform distribution of carbon nanotubes can be achieved in the polymer matrix by means of high shear stresses during mixing [14,15]. Adding various fibrous fillers can increase the apparent viscosity of the matrix to the desired extent and lead to a higher shear stress during processing, moreover they have a reinforcing effect themselves. In the past years a few researches dealt with these kind of hybrid composites, Karsli et al. observed synergistic effects on the tensile and impact properties of short glass fibre and carbon nanotube hybrid reinforced, injection moulded composites. Polyamide 6 (PA6) is one of the popular matrix materials for high performance composites as it can be effectively reinforced either with fibres or with nanoparticles, and these composites are well applicable for injection moulding. One of the most popular reinforcements for injection moulded polyamide matrix composites are short carbon fibres due to their low density, and high tensile strength and tensile modulus. Recently, a lot of promising carbon nanotube and carbon fibre reinforced, polyamide matrix hybrid composites have appeared, however most of these are based on growing the nanotubes onto the carbon fibres which makes their production expensive [16—21].

In case of a polyamide matrix nanocomposite, as being thermoplastic its long-term behaviour is another important issue, the nanotubes may effectively block the movement of the polymer chains that may decrease the creep significantly. Only a few studies have investigated the creep behaviour of carbon nanotube reinforced thermoplastic composites so far, and there has been even less research on hybrid composites. Jia et al. [22] observed, that adding 2.8 vol% carbon nanotube to the polypropylene matrix decreased the creep strain by 36%, even though the dispersion of the nanotubes was not uniform. As the hybrid reinforcement showed synergistic effect on the tensile and impact properties, it may have a positive effect also on the creep behaviour [22—26].

The main disadvantage of polyamide is moisture absorption, as its mechanical properties are highly dependent on the quantity of absorbed moisture. The moisture-dependent mechanical properties can be strongly influenced by the presence of reinforcing materials, especially in the case of nanocomposites, where the large surface of the particles results in a large interphase region. In this region, the polymer chains may be attached to the nanotubes which block the chain movement that results in lower crystallinity and ultimately, higher moisture absorption. If the nanotubes form larger aggregates, it may also block the crystallization and if the aggregates are not impregnated properly by the matrix, the capillary moisture absorption may also increase. On the other hand, the uniformly dispersed carbon nanotubes may act as crystal nucleation agents, and the higher crystallinity cause lower moisture absorption and better mechanical properties. Short carbon fibres may have a similar effect on the moisture absorption in PA matrix composites, and in the carbon fibre and carbon nanotube reinforced hybrid composites the combined effect of these reinforcements on the moisture absorption and its effect on the mechanical properties is not reported in the literature [27—33].

The aim of this research was to investigate the effect of the moisture content on the mechanical properties, namely the tensile and the creep behaviour of carbon fibre and carbon nanotube reinforced, polyamide 6 matrix composites that can be easily produced by extrusion and injection moulding.

2. Experimental

2.1. Materials

As matrix material, polyamide 6 homopolymer produced by A. Schulman GmbH (USA) was used (SHULAMID 6 MV 13 F, PA6). Its density was 1.13 g/cm^3 (at room temperature), and its melt flow index (MFI) was 14.7 g/10 min (2.16 kg, 230 °C). The carbon nanotubes were produced by Nanocyl s.a. (Belgium); the average diameter of the NANOCYL NC7000 carbon nanotubes (CNT) was 9.5 nm and their length was 1.5 μm. For fibre reinforcement, Panex 35 Chopped Pellet 95 carbon fibres were used (CF), produced by Zoltek Zrt. (Hungary). The fibres had an average starting length of 6 mm and diameter of 8.3 μm. The fibres had a density of 1.81 g/cm^3.

From the materials mentioned above, 10 different composite materials (Table 1) were prepared by extrusion on a Labtech LTE 26—44 type twin-screw extruder. Before

Table 1 — Components of the investigated composites.

Name	PA6 content [wt%]	CNT content [wt%]	Carbon fibre content [wt%]
PA6	100	0.00	0
PA6+0.25CNT	99.75	0.25	0
PA6+0.5CNT	99.50	0.50	0
PA6+0.75CNT	99.25	0.75	0
PA6+1CNT	99.00	1.00	0
PA6+30CF	70.00	0.00	30
PA6+30CF+0.25CNT	69.75	0.25	30
PA6+30CF+0.5CNT	69.50	0.50	30
PA6+30CF+0.75CNT	69.25	0.75	30
PA6+30CF+1CNT	69.00	1.00	30

extrusion, the PA6 granules were dried for 4 h at 80 °C in a Despatch LBB2-27-1CE type drying oven, then the raw materials were mechanically mixed at room temperature. Extrusion temperature was between 230 °C and 240 °C, and the speed of the screws was 25 1/min.

After extrusion, dumbbell type specimens with a cross-section of 4×10 mm² were injection moulded with an Arburg Allrounder 370 S 700−290 injection moulding machine (Germany). Melt temperature was between 255 °C and 275 °C, mould temperature was 80 °C and injection pressure was 1200 bar. The injection moulded specimens were conditioned in desiccators at 25 °C at 23.1% (distilled water + potassium acetate desiccant), 52.0% (distilled water + magnesium nitrate desiccant), 74.5% (distilled water + sodium chloride desiccant) and 99.9% (distilled water) for a month before testing.

2.2. Characterization methods

Tensile tests were carried out on at least 5 specimens/material on a Zwick Z005 universal testing machine (Germany) according to EN ISO 527. The tensile moduli were determined by the linear regression line fitted between the 0.05% and 0.25% displacement values. The tensile speed was 5 mm/min and gauge length was 110 mm.

Creep tests were carried out on at least 3 specimens/material on the same machine, the test load was approximately 30% of the tensile strength, which is still the linear viscoelastic range, but large enough to allow the differences to be well analysed [22,24,34]. In order to prove the linear viscoelasticity of the composites, pre-tests were carried out on the specimens conditioned at 100% relative humidity before the creep tests. During the pre-tests, the creep loads were 25%, 30% and 35% of the tensile strength. The creep compliance curves were coincident in the case of 25% and 30% loads, and higher creep compliance were observed in the case of 35% load. Therefore, 30% of the tensile strength was considered as the limit of the linear viscoelasticity. Based on the tensile tests, the test load was 17.5 MPa in the case of the pure, and CNT reinforced PA6, and 45 MPa for the CF reinforced and hybrid composites. To make these creep data comparable, the registered deformation−time plots were transformed to creep compliance−time plot, according to Equation (1).

$$J(t) = \frac{\varepsilon(t)}{\sigma_0} \tag{1}$$

where $\varepsilon(t)$ is the measured deformation as a function of time and σ_0 is the applied load. Testing time was 1200 s and the speed of uploading and unloading was 100 N/s.

According to the Burgers model, the total deformation (εt) of creep tested polymers can be divided into three components: the instantaneous elastic ($\varepsilon 0$), the time-dependent viscoelastic (ε_v) and the time-dependent viscous (or relaxation) deformation components (ε_r) (Fig. 1). Instantaneous elastic deformation is the initial deformation at $t = 0$. Viscoelastic deformation was determined by subtracting the instantaneous elastic deformation from the section of the $t = 0$ line and the tangent fitted to the endpoint of the creep curve. Viscous deformation was determined by subtracting the instantaneous elastic and the viscoelastic deformation from the total deformation [35−37].
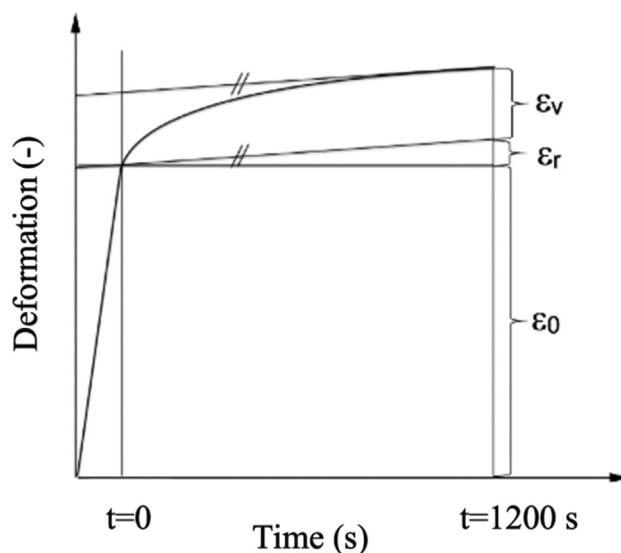

Fig. 1 − Determination of deformation components from the creep curves.

The fracture surfaces of the tensile tested specimens were inspected with a JEOL 6380 LA type scanning electron microscope (SEM), (Japan) after sputtering with gold.

Crystallinity was determined by thermal analysis performed on a TA Instruments Q2000 DSC machine (USA). The ~5 mg samples were cut out from the centre of the injection moulded dumbbell specimens, then heated to 240 °C, with a heating rate of 10 °C/min. In the crystallites, there are α and γ phases with different melting enthalpies. As their ratio is unknown, an average 240 J/g was considered to be the melting enthalpy of the 100% crystalline PA6 [38,39].

The moisture content of the matrix was determined by mass measurement, the mass of the conditioned dumbbell specimens were measured on a high-precision scale, then dried at 80 °C for 4 h, then measured again. The absorbed moisture contents of the specimens were calculated as follows:

$$A_m = \frac{W_c - W_d}{W_d \cdot (1 - \varphi)}$$

where A_m is the absorbed moisture, W_c is the weight of the conditioned and W_d is of the dried specimens and φ is the weight ratio of the reinforcement. From each material, 3-3 specimens were measured, the results were evaluated by statistical methods.

2.3. Results and discussion

2.3.1. Tensile tests

Tensile tests were carried out on specimens conditioned at 25%, 50%, 75% and 100% relative humidity. It can be seen in Table 2 that the tensile strength, the tensile modulus and the elongation at break of the composites reinforced only with carbon nanotubes decreased with increasing carbon nanotube content. The tensile strength and tensile modulus of the carbon fibre and carbon nanotube reinforced hybrid composites

Table 2 – Tensile properties of the composites.

Name	Tensile strength [MPa]	Standard deviation [MPa]	Tensile modulus [MPa]	Standard deviation [MPa]	Strain at break [%]	Standard deviation [%]
25% relative humidity						
PA	60.98	6.63	2.57	0.22	82.76	17.88
PA+0.25CNT	58.77	2.94	2.51	0.09	35.55	28.74
PA+0.5CNT	54.98	6.07	2.57	0.16	3.39	2.24
PA+0.75CNT	49.39	15.74	2.29	0.81	5.51	15.60
PA+1CNT	52.03	7.86	2.53	0.09	2.92	1.38
PA+30CF	173.33	7.35	12.15	0.80	3.45	0.89
PA+0.25CNT+30CF	172.56	4.69	12.21	0.93	3.47	0.28
PA+0.5CNT+30CF	178.50	4.03	12.85	0.87	3.13	0.45
PA+0.75CNT+30CF	177.87	2.66	12.56	0.38	3.21	0.39
PA+1CNT+30CF	177.19	5.74	12.56	2.48	3.87	2.86
50% relative humidity						
PA	58.90	8.00	2.10	0.14	105.95	138.83
PA+0.25CNT	50.24	13.08	1.98	0.09	21.39	32.75
PA+0.5CNT	43.39	14.33	2.10	0.02	4.72	13.68
PA+0.75CNT	45.80	9.34	2.09	0.07	6.26	14.11
PA+1CNT	47.77	15.15	2.14	0.04	8.89	19.25
PA+30CF	156.78	4.46	10.64	1.33	6.45	15.54
PA+0.25CNT+30CF	155.09	3.64	10.85	0.05	3.42	0.51
PA+0.5CNT+30CF	159.08	6.10	11.15	1.15	3.81	5.05
PA+0.75CNT+30CF	158.26	3.82	11.32	0.28	3.15	0.54
PA+1CNT+30CF	153.02	13.03	11.22	1.09	3.01	1.37
75% relative humidity						
PA	55.02	9.02	1.58	0.03	179.63	49.53
PA+0.25CNT	48.04	2.97	1.68	0.07	65.30	67.54
PA+0.5CNT	35.27	17.42	1.68	0.22	5.33	17.32
PA+0.75CNT	40.60	21.93	1.57	0.22	15.22	32.65
PA+1CNT	32.69	8.89	1.59	0.27	3.89	5.46
PA+30CF	140.10	8.36	10.04	1.34	3.64	0.45
PA+0.25CNT+30CF	141.14	1.66	10.43	1.03	3.39	0.52
PA+0.5CNT+30CF	146.34	3.05	10.63	0.91	3.34	1.22
PA+0.75CNT+30CF	142.54	6.71	10.16	1.63	2.99	1.06
PA+1CNT+30CF	142.49	5.59	10.12	1.97	3.03	0.53
100% relative humidity						
PA	54.15	128.43	1.41	0.02	210.89	82.73
PA+0.25CNT	31.22	23.15	1.35	0.06	8.32	25.82
PA+0.5CNT	32.11	28.86	1.34	0.06	12.15	50.00
PA+0.75CNT	29.18	23.46	1.35	0.06	8.18	33.96
PA+1CNT	31.39	56.88	1.02	1.70	46.07	124.36
PA+30CF	116.11	6.36	7.08	2.54	4.59	2.40
PA+0.25CNT+30CF	118.20	8.24	8.11	0.28	3.99	0.41
PA+0.5CNT+30CF	117.60	3.91	8.26	0.60	3.94	0.62
PA+0.75CNT+30CF	118.37	6.08	8.62	0.22	3.58	0.36
PA+1CNT+30CF	119.31	2.77	8.52	0.27	3.73	0.40

are higher than those of the composite containing only carbon fibres and increased with increasing nanotube content. Based on this and the SEM images discussed later, it can be concluded that adding carbon fibres to the composite resulted in a much more homogenous distribution of carbon nanotubes. The nanotubes were able to produce a reinforcing effect in the carbon fibre reinforced composite, in contrast to the composite reinforced only with nanotubes, where the large aggregates functioned as stress concentration centres.

The hybrid reinforcement had an advantageous effect also on the moisture dependent mechanical properties, in the presence of the carbon fibres the tensile strength and the modulus decreased to a lesser extent with the increasing moisture content, which effect intensified with the higher nanotube content. This is explained by the fact that in carbon fibre and carbon nanotube reinforced hybrid composites, the hydrophobic carbon fibres (which are 20 v% of the composite) are the primary load carriers and the failure of the softening matrix due to the moisture content is less significant. In the hybrid composites, the nanotubes are dispersed uniformly, and as a result, a higher fraction of polymer chains are immobilized by them, which compensate the softening effect of moisture.

2.3.2. SEM images

Figure 2 a shows the ductile fracture surface of the reference PA6, which is typical for polyamides with high modulus and strain at break. However, the fracture surfaces of the nanotube reinforced composites (Fig. 2 b-e) a show a much less ductile behaviour, and it is well noticeable that the starting point of failure is an aggregate of about 200–300 μm in diameter. Based on SEM images and tensile properties, it can
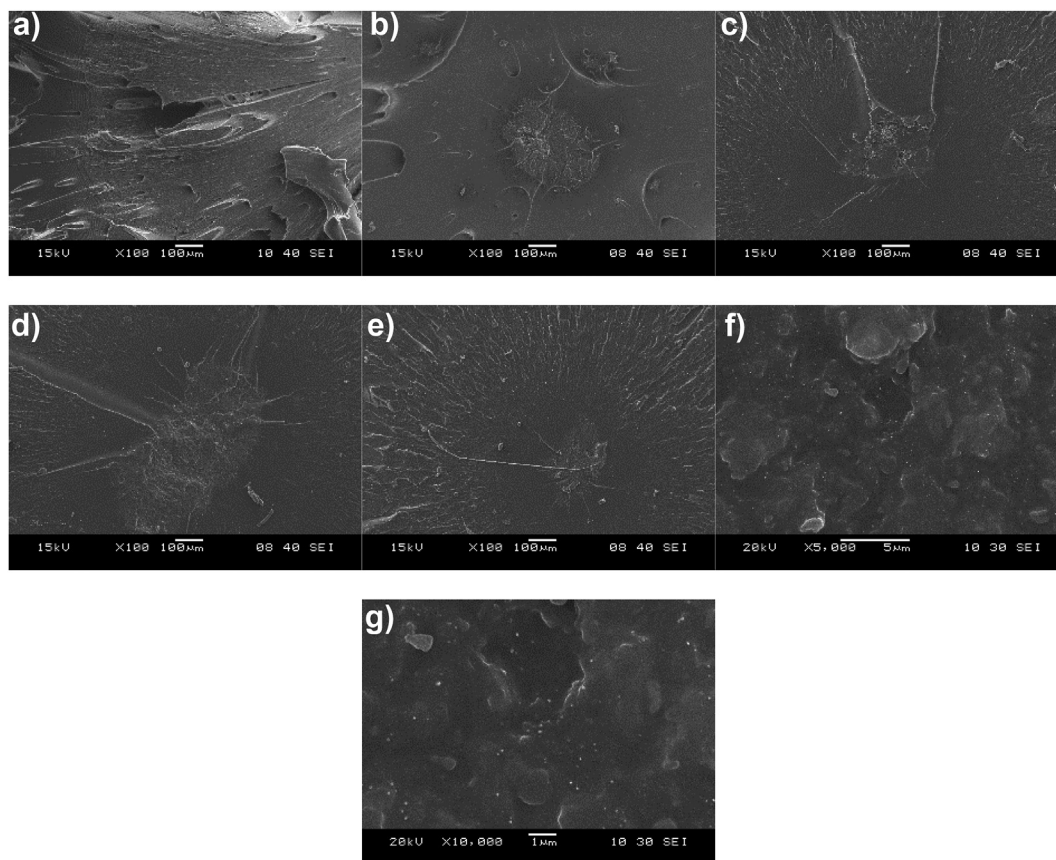
Fig. 2 – SEM images of the nanocomposites (25% RH): a) pure PA6, b) PA6+0.25 CNT, c) PA6+0.75CNT, d) PA6+1CNT, e)-g) PA6+0.5CNT.

be assumed that instead of reinforcing, CNTs created a stress concentration centre in the composite. The analysis of aggregates at higher magnification shows that the aggregates were impregnated by the matrix satisfactorily (Fig. 2 f, g), moreover, uniformly dispersed, single nanotubes can also be found near the aggregates, but the effect of the aggregates on the mechanical properties was dominant. A similar structure was found in composites with a carbon nanotube content of 0.5 m%, 0.75 m% and 1 m%.

On the fracture surface of the composites containing 30 m % carbon fibres (Fig. 3 a), the starting point for failure cannot be clearly identified, moreover large amount of broken fibres can be observed. The hybrid composites show a similar fracture surface (Fig. 3 b), that suggests that failure was not caused by large aggregates of carbon nanotubes. A magnification of 5000× did not show any CNT aggregates on the surface of the sample, and mostly single nanotubes are recognizable, which indicates their uniform dispersion (Fig. 3 c-f).

2.3.3. The effect of nanotube content on moisture absorption and crystallinity

Figure 4 a shows that the moisture absorption of the carbon nanotube reinforced composites slightly increased with the increase of the carbon nanotube content, and this increasing became significant at larger relative humidity. This may indicate that the higher nanotube content increased the influence of relative humidity, and this may be reflected in the mechanical properties of the composites. Fig. 4 b shows the moisture absorption of the hybrid composites reinforced with carbon fibre and carbon nanotubes. Increasing the carbon nanotube content did not lead to a significant increase of moisture absorption. To detect the causes for this, DSC tests were carried out to investigate crystallinity, as the reinforcing materials have an effect on the morphology of the matrix, and this may influence moisture absorption.

It can be seen on Fig. 5 that the crystallinity of the only carbon nanotube reinforced composites, decreased as carbon nanotube content increased, and this is strongly related to increasing moisture absorption, as in the polymer matrix only the amorphous parts can absorb moisture. The lower crystallinity of the only carbon nanotube reinforced composite may be explained by that the nanotubes hindered effectively the movement of the polymer chains, that did not allow them to form a crystalline structure. Additionally, the nanotubes improved the thermal conductivity of the composites, the solidification from melt was faster, and only a shorter period of time was available for the crystallization (see Fig. 6).

In the case of composites reinforced with carbon fibres and carbon nanotubes, crystallinity dropped only by 2.3%, while it dropped by 2.6% in composites reinforced only with carbon nanotubes. In the hybrid composites the dispersion of the nanotubes was much more uniform, thus their heterogeneous
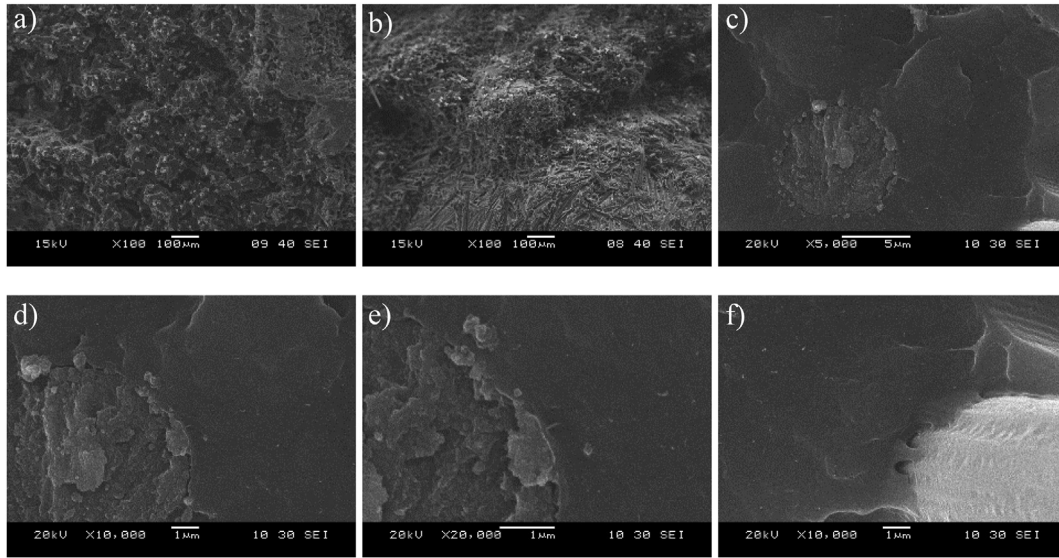
Fig. 3 − SEM images of the hybrid nanocomposites (25% RH): a) only CF reinforced PA6, b) -f) PA6+30CF+0.5CNT.

crystalline nucleating effect became more significant compared to the formerly mentioned chain mobility decreasing effects.

2.3.4. Creep tests

The tensile tests showed that hybrid composites performed well and showed synergistic effects as expected, but in the case of composites containing only nanotubes, the reinforcing role of nanoparticles was less effective. Similar results may be observed on the creep compliance curves (Fig. 6) of the pure PA6, and the CNT reinforced composites.

The carbon fibres have a high elastic modulus, which significantly decreases the instantaneous elastic creep compliance. In order to better understand the structure-related creep behaviour of the composites, the time-dependent part of the creep data should be investigated, for which the instantaneous elastic creep compliance is subtracted from the creep compliance curves (Fig. 7).

It is well noticeable that the time-dependent creep compliance of the pure PA was the smallest, while it was larger in the carbon nanotube reinforced composites for each nanotube content (Fig. 7). No clear relationship could be observed between carbon nanotube content and the magnitude of creep compliance. The reason for this may be that the aggregates are loose structures of adhered nanotubes that are deformed more than the matrix under constant load [26]. Deformation is significantly determined by the size and distribution of the aggregates, which are mainly influenced by the melt flow processes that are difficult to determine and control during processing (e.g. the melt viscosity is much higher in the interphase between the matrix and the nanotubes), and the effect of carbon nanotubes is significantly lower. However, in tensile tests, it was observed that tensile strength and modulus, and elongation at break decreased when carbon nanotube content increased. The explanation for the difference between the tensile and the creep properties
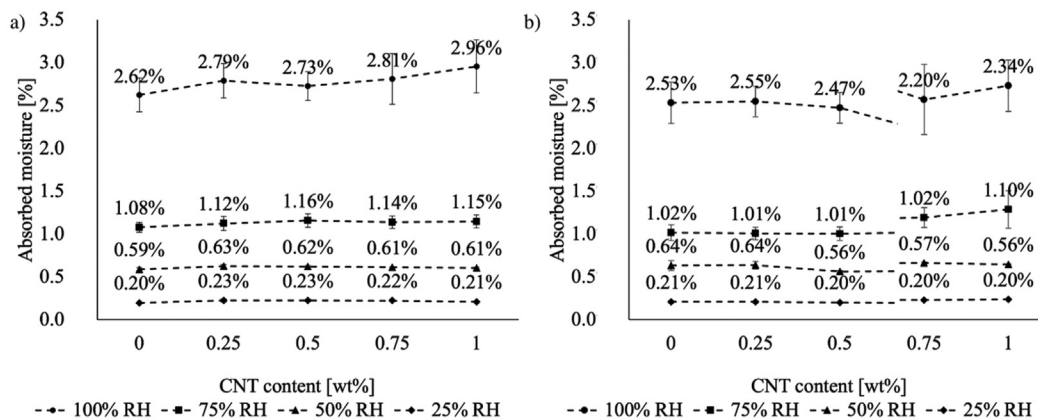

Fig. 4 − Moisture absorption of the matrix a) of the only carbon nanotube reinforced composites, b) of the carbon fibre and carbon nanotube reinforced composites.
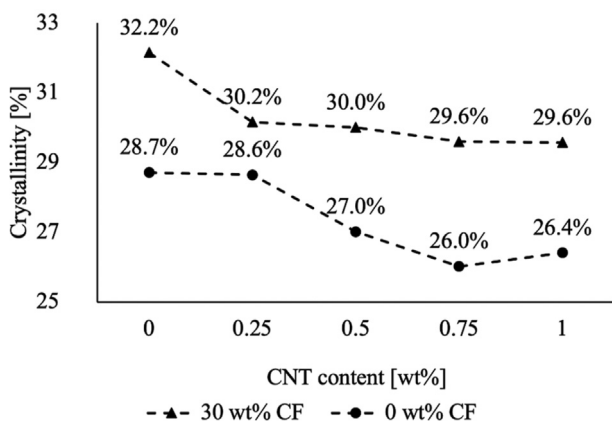
Fig. 5 – Crystallinity of the composites.

is that during tensile tests the modulus is valid for initial small deformations (linear elastic region) and the tensile strength at the moment of failure, but the creep test occurs in the linear viscoelastic region between them. Deformation speed may also affect the mechanical properties: while the tensile tests had a deformation speed of 5 mm/min, it was on average an order of magnitude lower during the creep tests.

The carbon fibres obviously had a positive effect on the creep behaviour of the composites containing nanotubes and carbon fibres (Fig. 7): the time-dependent creep compliance of the composite reinforced only with carbon fibres was lower than that of the pure PA6 or any of the composites reinforced with only carbon nanotubes. Adding carbon nanotubes to the composite besides the carbon fibres reduced creep compliance of the composites even more; and it decreased significantly as nanotube content increased. Similar creep

behaviour and trends were obtained in the 50%, 75% and 100% relative humidity conditions tested.

The hybrid reinforcement was advantageous for the moisture dependent creep behaviour, the hybrid composite reinforced with 30 wt% carbon fibre and 0.5 wt% carbon nanotubes (Fig. 8, black curves) showed a higher creep compliance with increasing humidity, but the effect of humidity here was much less significant than in the case of the 0.5 wt% carbon nanotube reinforced composite (Fig. 8, grey curves). The carbon fibres facilitated the uniform distribution of the nanotubes, therefore crystallization was hampered less by the nanotube aggregates. Because of this, the increasing nanotube content resulted in a slighter decrease in crystallinity, thus a much smaller increase in creep deformation.

Figure 9 shows that higher nanotube content resulted in higher instantaneous elastic (a) and lower viscous (b) deformation. The increasing instantaneous elastic deformation of the nanocomposite suggests that in the composite, besides the stochastically distributed aggregates, uniformly dispersed nanotubes were present, which adhere well to the matrix (Fig. 2). A decline in the viscous deformation component suggests that nanotubes adhered adequately to the PA matrix without special surface treatment and effectively hindered the movement of the polymer chains [26].

Figure 9 b shows that higher humidity resulted in greater viscous deformation: the viscous deformation increased from 8.7% to 14.9% of total deformation, while instantaneous deformation decreased from 67% to 48.9% in the case of pure PA6. With increasing moisture content, instantaneous elastic deformation decreased, while viscous deformation became more dominant, and this trend was strengthened by the presence of the nanotubes. The reason for this is that according to the DSC
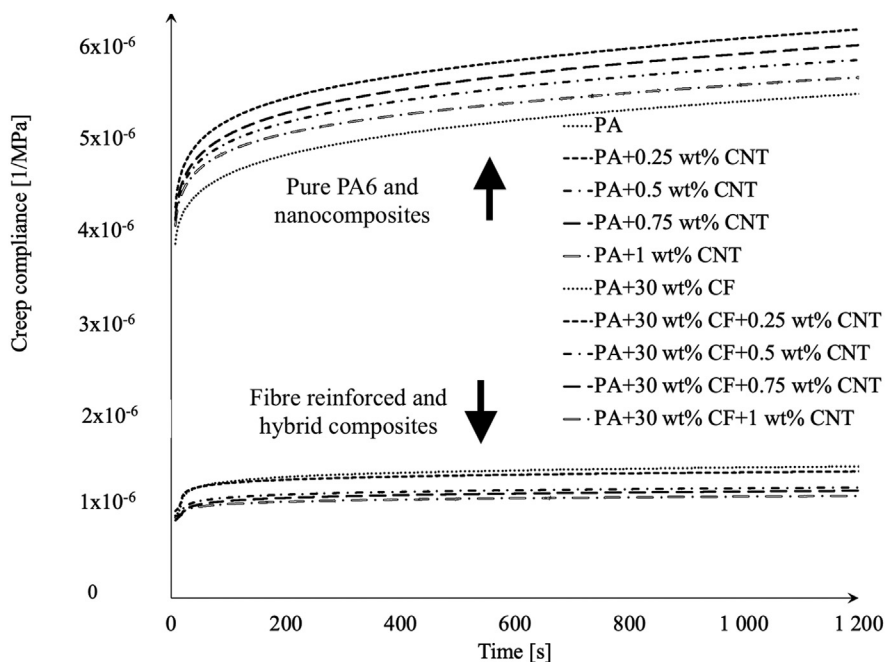

Fig. 6 – Creep compliances of the nano- and hybrid composites conditioned at 25% RH.
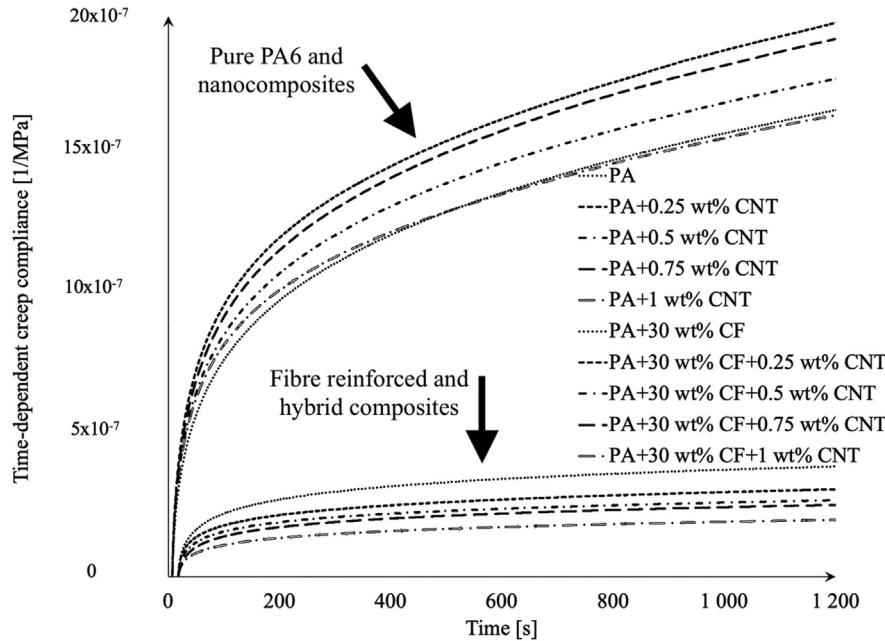
Fig. 7 – Time-dependent creep compliances of the nano- and hybrid composites conditioned at 25% RH.

tests, increasing nanotube content resulted in lower crystallinity, and as crystalline parts cannot absorb moisture, moisture absorption increased with increasing nanotube content. Therefore, an increase in carbon nanotube content may increase the softening effect of moisture.

In the hybrid composites, the presence of carbon nanotubes had an advantageous effect on the moisture sensitivity of the composites, as nanotube content increased, the ratio of the instantaneous elastic deformation increased significantly (Fig. 10 a), while the ratio of viscous deformation decreased (Fig. 10 b). This indicates that the uniformly dispersed carbon nanotubes properly adhered to the matrix and effectively reduced the mobility of the polymer chains, thereby an

interphase was created around the nanotubes, which had an additional reinforcing effect.

According to the principle of moisture content–time superposition, under constant load, increase in the absorbed moisture of a material produces a similar effect in a longer load time, i.e. viscous deformation increases, and instantaneous deformation decreases [40]. As viscous deformation does not increase at high humidity as much as in case of the polyamide reinforced only with carbon fibres, due to the presence of nanotubes, it can be concluded that at lower humidity content (which is close to the operational conditions of the composite) deformation remains low even at a long-time load.
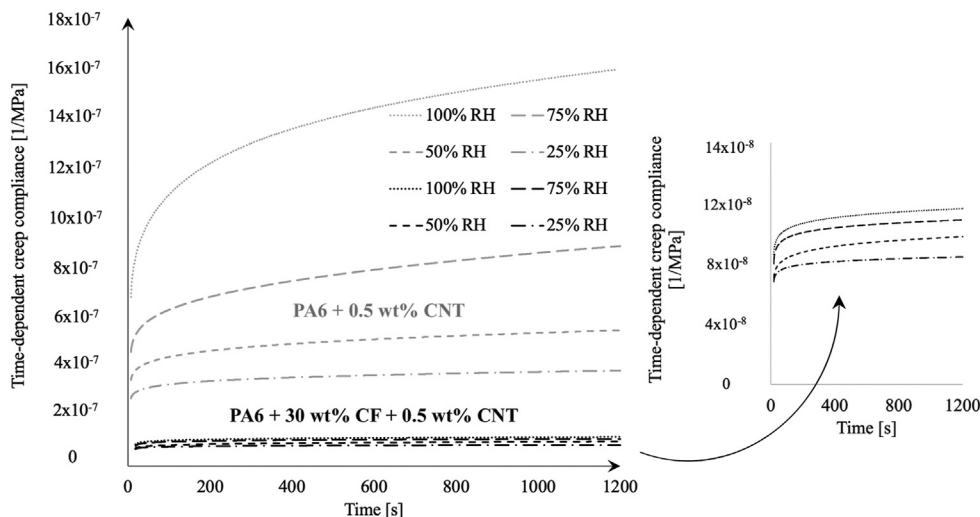

Fig. 8 – Time-dependent creep compliances of the nano- and hybrid composites conditioned at different relative humidities.
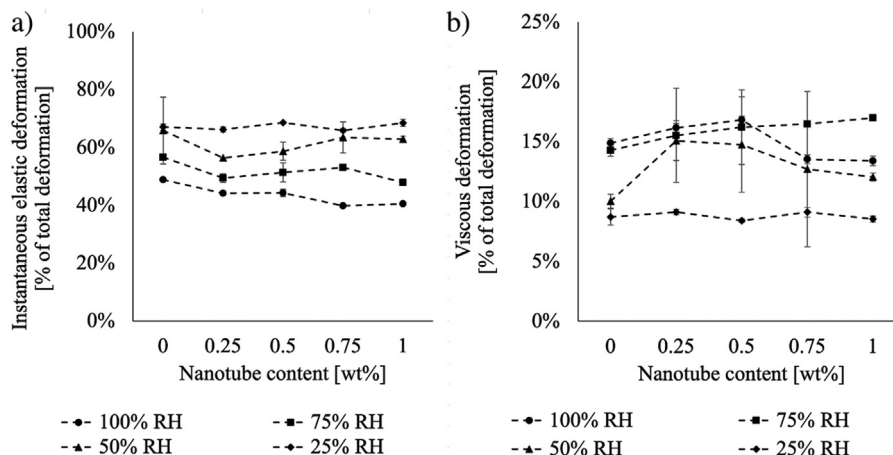
Fig. 9 − a) Instantaneous elastic deformation, b) viscous deformation of the composites reinforced with only carbon nanotubes.
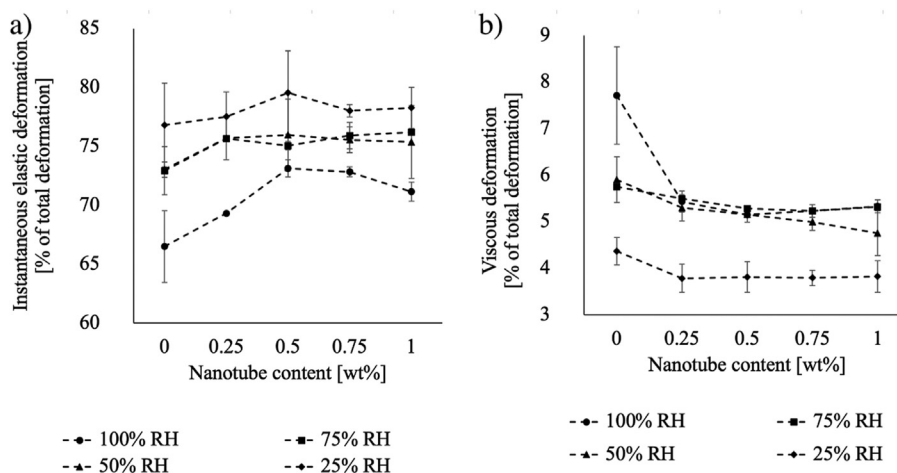

Fig. 10 − a) Instantaneous elastic deformation, b) viscous deformation of the composites reinforced with carbon nanotubes and carbon fibres.

3. Conclusions

We investigated the long-term mechanical behaviour of carbon nanotube reinforced composites and carbon nanotube and carbon fibre reinforced hybrid composites. The effect of the relative humidity of the environment on the mechanical behaviour of the composites was also investigated.

We found that carbon fibres and carbon nanotubes have a synergistic effect on the mechanical properties of the composite. Adding carbon nanotubes to the carbon fibre reinforced composites improved the mechanical properties compared to composites containing only carbon fibres.

In the SEM images, it was observed that in the composites containing only carbon nanotubes, failure was initialized in all cases by a larger aggregate. No visible aggregates were found in the carbon fibre reinforced hybrid composites, only uniformly dispersed, single nanotubes among the carbon fibres.

The increase of nanotube content resulted in higher moisture absorption. However, in the case of the carbon fibre and carbon nanotube reinforced composite, this increase was much less significant. According to the DSC tests, higher moisture absorption was caused by the lower crystallinity of the nanotube-reinforced composites.

Adding carbon nanotubes made the elongation of the composites at constant loads greater than that of pure PA in the creep tests. The increasing nanotube content resulted in smaller viscous and larger instantaneous elastic deformation. Moisture content had a significant effect on the creep properties; in the case of composites reinforced only with carbon nanotubes, nanotube content increased the influence of moisture content, thus decreased instantaneous elastic deformation and increased viscous deformation. In the case of the hybrid composites containing carbon fibres, it was observed that total deformation decreased, and instantaneous elastic deformation increased with the increase in

nanoparticle content. This indicates that the nanotubes were homogenously dispersed in the composite; they adhere well to the PA6 and effectively block the movement of polymer chains. Moisture content had much less influence on the creep behaviour of the hybrid composites; the decrease of instantaneous elastic deformation and the increase in viscous deformation was much lower. In sum, carbon fibre and carbon nanotube reinforced hybrid composites are less sensitive to moisture content and have a more advantageous long-time behaviour than composites reinforced with only nanotubes.

Funding

Authors' contributions

Roland Petrény is the first author of this study and was responsible for performing the experiments and for collecting and analysing the data. László Mészáros, the second and corresponding author, was responsible for the literature review and for planning the experiments. Both the authors equally contributed to the preparation of the manuscript including graphs and figures. All authors have read and approved the final manuscript.

Declaration of Competing Interest

The authors declare that they have no known competing financial interests or personal relationships that could have appeared to influence the work reported in this paper.

REFERENCES

[1] Andrews R, Weisenberger MC. Carbon nanotube polymer composites. Curr Opin Solid State Mater Sci 2004;8(1):31–7. https://doi.org/10.1016/j.cossms.2003.10.006.

[2] Suprakas Sinha Ray MB. Polymer nanocomposites and their applications. Canada: Department of Chemical Engineering, Laval University; 2006.

[3] Anandhan Sb S. Polymer nanocomposites: from synthesis to applications. InTech; 2011. doi:10.5772/17039.

[4] Jalalvand M, Czél G, Wisnom MR. Damage analysis of pseudo-ductile thin-ply UD hybrid composites — a new analytical method. Compos Appl Sci Manuf 2015;69:83–93. https://doi.org/10.1016/j.compositesa.2014.11.006.

[5] Zoltán J, Tamás T, Tamás Bence T, András S. Sensitivity analysis for frequency based prediction of crack size in composite plates with through-the-width delamination. Int J Damage Mech 2017. https://doi.org/10.1177/1056789517709893. 1056789517709893.

[6] Yu Ol MF, Dyer MJ, Moloni K, Kelly TF, Ruoff RS. Strength and breaking mechanism of multiwalled carbon nanotubes under tensile load. Science 2000;287:637–40.

[7] Zhang S, Park JG, Nguyen N, Jolowsky C, Hao A, Liang R. Ultra-high conductivity and metallic conduction mechanism of scale-up continuous carbon nanotube sheets by mechanical stretching and stable chemical doping. Carbon N Y 2017;125:649–58. https://doi.org/https://doi.org/10.1016/j.carbon.2017.09.089.

[8] Gojny FH, Wichmann MHG, Fiedler B, Schulte K. Influence of different carbon nanotubes on the mechanical properties of epoxy matrix composites — a comparative study. Compos Sci Technol 2005;65(15):2300–13. https://doi.org/10.1016/j.compscitech.2005.04.021.

[9] Thostenson ET, Ren Z, Chou T-W. Advances in the science and technology of carbon nanotubes and their composites: a review. Compos Sci Technol 2001;61(13):1899–912. https://doi.org/10.1016/S0266-3538(01)00094-X.

[10] Vahid T. An elasticity solution for vibration analysis of laminated plates with functionally graded core reinforced by multi-walled carbon nanotubes. Period Polytech - Mech Eng 2017;61:309–19. https://doi.org/10.3311/PPme.11254.

[11] Ryu J, Han M. Improvement of the mechanical and electrical properties of polyamide 6 nanocomposites by non-covalent functionalization of multi-walled carbon nanotubes. Compos Sci Technol 2014;102:169–75. https://doi.org/10.1016/j.compscitech.2014.07.022.

[12] Zhang S, Ma Y, Suresh L, Hao A, Bick M, Tan SC, et al. Carbon nanotube reinforced strong carbon matrix composites. ACS Nano 2020;14:9282–319. https://doi.org/10.1021/acsnano.0c03268.

[13] Wu CS, Liao HT. Interface design of environmentally friendly carbon nanotube-filled polyester composites: fabrication, characterisation, functionality and application. Express Polym Lett 2017;11:187–98. https://doi.org/10.3144/expresspolymlett.2017.20.

[14] Mack C, Sathyanarayana S, Weiss P, Mikonsaari I, Hübner C, Henning F, et al. Twin-screw extrusion of multi walled carbon nanotubes reinforced polycarbonate composites: investigation of electrical and mechanical properties. IOP Conf Ser Mater Sci Eng 2012;40(1):012020.

[15] Margolis JM. Conductive polymers and plastics. New York: Chapman & Hall; 1989.

[16] Ma Y, Jin S, Zhang S. Effect of trigger on crashworthiness of unidirectional carbon fibre reinforced polyamide 6 composites. Plast Rubber Compos 2018;47:208–20. https://doi.org/10.1080/14658011.2018.1466502.

[17] Gamze Karsli N, Yesil S, Aytac A. Effect of hybrid carbon nanotube/short glass fiber reinforcement on the properties of polypropylene composites. Compos B Eng 2014;63:154–60. https://doi.org/10.1016/j.compositesb.2014.04.006.

[18] Yourdkhani M, Liu W, Baril-Gosselin S, Robitaille F, Hubert P. Carbon nanotube-reinforced carbon fibre-epoxy composites manufactured by resin film infusion. Compos Sci Technol 2018. https://doi.org/10.1016/j.compscitech.2018.01.006.

[19] He Y, Yang S, Liu H, Shao Q, Chen Q, Lu C, et al. Reinforced carbon fiber laminates with oriented carbon nanotube epoxy nanocomposites: magnetic field assisted alignment and cryogenic temperature mechanical properties. J Colloid Interface Sci 2018;517:40–51. https://doi.org/10.1016/j.jcis.2018.01.087.

[20] Munoz-Velez MF, Valadez-Gonzalez A, Herrera-Franco PJ. Effect of fiber surface treatment on the incorporation of carbon nanotubes and on the micromechanical properties of a single-carbon fiber-epoxy matrix composite. Express Polym Lett 2017;11:704–18. https://doi.org/10.3144/expresspolymlett.2017.68.

[21] Zhang L, De Greef N, Kalinka G, Van Bilzen B, Locquet J-P, Verpoest I, et al. Carbon nanotube-grafted carbon fiber polymer composites: damage characterization on the micro-scale. Compos B Eng 2017;126:202–10. https://doi.org/10.1016/j.compositesb.2017.06.004.

[22] Jia Y, Peng K, Gong X-l, Zhang Z. Creep and recovery of polypropylene/carbon nanotube composites. Int J Plast 2011;27(8):1239–51. https://doi.org/10.1016/j.ijplas.2011.02.004.

[23] Ansari R, Hassanzadeh-Aghdam MK. Micromechanical investigation of creep-recovery behavior of carbon nanotube-reinforced polymer nanocomposites. Int J Mech Sci 2016;115–116:45–55. https://doi.org/10.1016/j.ijmecsci.2016.06.005.

[24] Jia Y. Creep of thermoplastic polyurethane reinforced with ozone functionalized carbon nanotubes. Express Polym Lett 2012;6:750–8. https://doi.org/10.3144/expresspolymlett.2012.80.

[25] Mészáros L, Deák T, Balogh G, Czvikovszky T, Czigány T. Preparation and mechanical properties of injection moulded polyamide 6 matrix hybrid nanocomposite. Compos Sci Technol 2013;75:22–7. https://doi.org/10.1016/j.compscitech.2012.11.013.

[26] Szakács J, Mészáros L. Synergistic effects of carbon nanotubes on the mechanical properties of basalt and carbon fiber-reinforced polyamide 6 hybrid composites. J Thermoplast Compos Mater 2017;31(4):553–71. https://doi.org/10.1177/0892705717713055.

[27] Chung DDL, Chung D. Carbon fiber composites. Elsevier Science; 2012.

[28] Morgan P. Carbon fibers and their composites. Boca Raton: CRC Press; 2005.

[29] Lasoski SW, Cobbs WH. Moisture permeability of polymers. I. Role of crystallinity and orientation. J Polym Sci 1959;36(130):21–33. https://doi.org/10.1002/pol.1959.1203613003.

[30] Eitan A, Fisher FT, Andrews R, Brinson LC, Schadler LS. Reinforcement mechanisms in MWCNT-filled polycarbonate. Compos Sci Technol 2006;66(9):1162–73. https://doi.org/10.1016/j.compscitech.2005.10.004.

[31] Sje K. Cooling rate dependence of the crystallinity at nonisothermal crystallization of polymers: a phenomenological model. J Appl Polym Sci 2016;133(6). https://doi.org/10.1002/app.42977.

[32] Frihi D, Layachi A, Gherib S, Stoclet G, Masenelli-Varlot K, Satha H, et al. Crystallization of glass-fiber-reinforced polyamide 66 composites: influence of glass-fiber content and cooling rate. Compos Sci Technol 2016;130:70–7. https://doi.org/10.1016/j.compscitech.2016.05.007.

[33] Valentini L, Biagiotti J, López-Manchado MA, Santucci S, Kenny JM. Effects of carbon nanotubes on the crystallization behavior of polypropylene. Polym Eng Sci 2004;44(2):303–11. https://doi.org/10.1002/pen.20028.

[34] Starkova O, Buschhorn ST, Mannov E, Schulte K, Aniskevich A. Creep and recovery of epoxy/MWCNT nanocomposites. Compos Appl Sci Manuf 2012;43(8):1212–8. https://doi.org/10.1016/j.compositesa.2012.03.015.

[35] Behbahani H, Ziari H, Kamboozia N. Evaluation of the visco-elasto-plastic behavior of glasphalt mixtures through generalized and classic Burger's models modification. Construct Build Mater 2016;118:36–42. https://doi.org/10.1016/j.conbuildmat.2016.04.157.

[36] Hossain MI, Faisal HM, Tarefder RA. Determining effects of moisture in mastic materials using nanoindentation. Mater Struct 2016;49(3):1079–92. https://doi.org/10.1617/s11527-015-0559-9.

[37] Kumar R, Saboo N, Kumar P, Chandra S. Effect of warm mix additives on creep and recovery response of conventional and polymer modified asphalt binders. Construct Build Mater 2017;138:352–62. https://doi.org/10.1016/j.conbuildmat.2017.02.019.

[38] Millot C, Fillot L-A, Lame O, Sotta P, Seguela R. Assessment of polyamide-6 crystallinity by DSC. J Therm Anal Calorim 2015;122(1):307–14. https://doi.org/10.1007/s10973-015-4670-5.

[39] Fornes TD, Paul DR. Crystallization behavior of nylon 6 nanocomposites. Polymer 2003;44(14):3945–61. https://doi.org/10.1016/S0032-3861(03)00344-6.

[40] Maksimov RD, Mochalov VP, Urzhumtsev YS. Time — moisture superposition. Polym Mech 1972;8(5):685–9. https://doi.org/10.1007/BF00856097.